Available online at www.sciencedirect.com

SCIENCE @ DIRECT®

Polymer 45 (2004) 1805–1814

polymer

www.elsevier.com/locate/polymer

Polyethercarbonate–silica nanocomposites synthesized by copolymerization of allyl glycidyl ether with CO_2 followed by sol–gel process

Chung-Sung Tan*, Chun-Chieh Juan, Ting-Wu Kuo

Department of Chemical Engineering, National Tsing Hua University, Hsinchu 30043, Taiwan, ROC

Received 7 October 2003; received in revised form 25 December 2003; accepted 5 January 2004

Abstract

The catalyst system consisting of $Y(CF_3CO_2)_3$, $Zn(Et)_2$, and pyrogallol in the solvent of 1,3-dioxolane was found to be effective for the copolymerization of allyl glycidyl ether with carbon dioxide at 60 °C and 400 psi. The IR, ^{1}H-NMR, and ^{13}C-NMR spectra as well as the element analysis indicated that the resulting copolymer was an alternating polyethercarbonate with the carbonate content higher than 97.5%. The resulting polyethercarbonate could react with 3-(trimethoxysilyl)propyl methacrylate via a free radical reaction to generate the alkoxysilane-containing copolymer precursors that were used in the subsequent sol–gel process to result in the polyethercarbonate–silica nanocomposite. The generated nanocomposite was characterized by ^{13}C-NMR, ^{29}Si-NMR, SEM, DSC, TGA, ESCA, and UV–Vis. The mechanical properties were also measured. A good compatibility between polyethercarbonate and silica and a SiO_2 network with silica particles less than 100 nm in the nanocomposite were observed. Both the thermal and mechanical properties of the resulting polyethercarbonate–silica nanocomposite were found to enhance with silica content. The optical transparency of the generated nanocomposite was comparable to that of the based polyethercarbonate.

Keywords: Carbon dioxide; Polyethercarbonate; Nanocomposite

1. Introduction

Because carbon dioxide (CO_2) is readily available, inexpensive, nontoxic, and nonflammable, it can be used as the starting monomer to substitute toxic monomers for synthesis of polycarbonate [1–3]. But due to its inert nature, a catalyst is generally required to proceed this kind of polymerizations. Recently, rare-earth metal coordination catalysts have been proved to be effective in the synthesis of polyethercarbonate from CO_2 and epoxide [4–8]. While a high molecular weight and a high carbonate content of aliphatic polyethercarbonate, such as poly(propylene carbonate), could be generated, its application has the limitations due to its low thermal and mechanical stabilities. Though the thermal and mechanical properties can be improved using cyclic epoxides, such as cyclohexene oxide, as the monomers, brittleness and poor transparency are the major drawbacks for the resulting cyclic polyethercarbonates.

Polymer–inorganic nanocomposites prepared by the sol–gel process have attracted a great attention in the past years [9–14]. One of the major advantages of a sol–gel process is its low temperature and pressure operation. The thermal and mechanical properties of the resulting nanocomposites are in general influenced by particle sizes and interaction between the dispersed and continuous phases. It has been revealed that the properties of the resulting polymer–SiO_2 nanocomposite can be much improved compared to the parent polymers. Tetraethoxysilane (TEOS) and tetramethoxysilane (TMOS) are the common sol–gel materials. Obviously, the synthesis of a polyethercarbonate–SiO_2 nanocomposite is an alterative means to improve thermal and mechanical properties of a polyethercarbonate itself. In the synthesis, a chemical bond between organic and inorganic constituents is usually preferred to avoid macroscopic phase separation. To achieve this purpose, an aliphatic epoxide with allyl groups may be a

---

* Corresponding author. Tel.: +886-3-5721189; fax: +886-3-5721684.
E-mail address: cstan@che.nthu.edu.tw (C.S. Tan).

0032-3861/$ - see front matter © 2004 Elsevier Ltd. All rights reserved.
doi:10.1016/j.polymer.2004.01.013

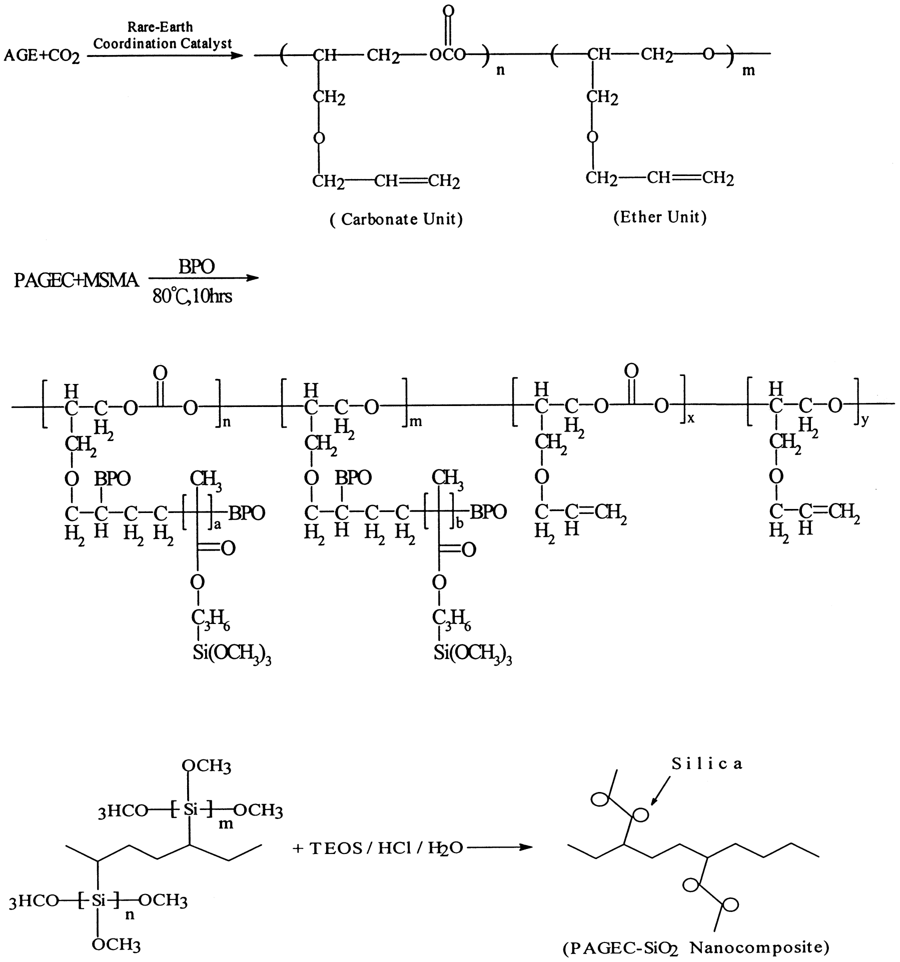

Scheme 1.

candidate in copolymerization. Lukaszczyk et al. [15] successfully synthesized a polyethercarbonate from the copolymerization of allyl glycidyl ether (AGE) with CO_2 using the catalyst diethyl zinc and pyrogallol. The molecular weight of the resulting copolymer could be as high as 1.0×10^6, but the thermal and mechanical properties were not reported.

The objective of this study is to systematically study the copolymerization of AGE with CO_2 using the yttrium metal coordination catalyst systems previously used for aliphatic and cyclic copolymerization [6,7]. The molecular weight and its distribution, thermal, and mechanical properties of the resulting poly(AGE carbonate) (PAGEC) were measured to determine the most appropriate operating conditions for the copolymerization. The copolymer precursors possessing trimethoxysilyl functional group were prepared by the free radical reaction of PAGEC with 3-(trimethoxysilyl)propyl methacrylate (MSMA), vinyltriethoxysilane (VTES), or vinyltrimethoxysilane (VTMS) using benzoyl peroxide (BPO) as the initiator. The sol–gel method was then used to generate PAGEC–SiO_2 nanocomposites by adding TEOS in the presence of the catalyst HCl. The thermal and mechanical properties of the generated nanocomposites were measured and compared with those of the PAGEC. The reaction schemes for the synthesis of PAGEC–SiO_2 nanocomposites are summarized as follows (Scheme 1).

2. Experimental

2.1. Materials

AGE of a purity of 99% (Tokyo Chemical Industry) was refluxed over CaH_2 for 4 h and then distilled before use. Diethylzinc ($Zn(Et)_2$), glycerine, TEOS, MSMA, VTES, VTMS, and all the solvents including D-chloroform, 1,3-dioxolane, ethanol, *n*-hexane, and tetrahydrofuran (THF) were of analytical regent grade and were used without further purification. Carbon dioxide of a 99.99% purity (Air Product) was used as received. Yttrium trifluoroacetate $Y(CF_3CO_2)_3$ and pyrogallol were heated in vacuum at 80 °C for 40 h and BPO was recrystallized from acetone before use.

The catalyst system containing $Y(CF_3CO_2)_3$ (I), $Zn(Et)_2$ (II), and pyrogallol (III) was prepared in an atmosphere of argon. The preparation was done by dissolving pyrogallol in a solvent. The resultant solution was then added dropwise to the solution of $Zn(Et)_2$ and the same solvent at room temperature. After heating the solution containing suspended powers resulted from $Zn(Et)_2$ and pyrogallol for 2 h, it was added to a 300 ml autoclave equipped with a magnetic stirrer (Autoclave Engineers Inc.) in which a known amount of $Y(CF_3CO_2)_3$ was present. Before the addition of the solution, the autoclave was heated in vacuum at 100 °C for 4 h in order to remove oxygen and moisture. The resultant yttrium-metal catalyst solution was stirred at 60 °C for 1 h before CO_2 and epoxide were introduced.

2.2. Copolymerization

The copolymerization of AGE with CO_2 was carried out in a 300 ml autoclave that was equipped with a magnetic stirrer (Autoclave Engineers Inc.) and loaded with the prepared catalyst system at a spinning speed of 1000 rpm. After a certain period of reaction time, the pressure was reduced to atmosphere to terminate the copolymerization and an excess of aqueous methanol solution containing dilute hydrochloric acid (10 wt%) was added to result in a precipitation of the copolymer. The precipitated crude copolymer was purified by dissolving it in THF first and then being precipitated again by the addition of a 50 wt% aqueous methanol solution. After three times purification treatment, the copolymer PAGEC was dried under vacuum at 40 °C for 8 h prior to analysis.

2.3. Preparation of the PAGEC–$Si(OCH_3)_3$ precursor

To prepare the copolymer precursor PAGEC–$Si(OCH_3)_3$ for the sol–gel process, 3.0 g of PAGEC was allowed to react with MSMA, VTES, or VTMS in a 120 ml of THF at 80 °C under nitrogen for 10 h. In the preparation, the amounts of MSMA, VTES, and VTMS added were varied from 4.7×10^{-3} to 1.9×10^{-2} mol and BPO about 1.0 mol% of the silicon content compound was used as the free radical initiator. The resultant copolymer precursor was purified by the reprecipitation in hexane. After three times purification treatment, the copolymer precursor was dried under vacuum at 40 °C for 4 h.

2.4. Preparation of the PAGEC–SiO_2 nanocomposite

The PAGEC–SiO_2 nanocomposites were synthesized via a sol–gel process. In the synthesis, a solution denoted as Sol-A was prepared by dissolving the copolymer precursor in THF, and another solution denoted as Sol-B was prepared by stirring vigorously a THF solution containing a certain amount of TEOS and 0.2 M of HCl. The Sol-A and Sol-B were then mixed in a beaker under vigorous stirring for 10 min to result in a clear homogeneous solution. After that, this solution was allowed to evaporate THF and the low molecular weight products such as methanol, ethanol, and water resulting from hydrolysis and condensation at room temperature until the formation of a clear gel. The clear gel was then cast onto a Teflon-coated plate. After drying the plate for 7–8 days at 30 °C, a transparent film of the PAGEC–SiO_2 nanocomposite was generated.

2.5. Instrumentation and characterization

The ^1H-NMR and ^{13}C-NMR spectra were recorded with a Varian spectrometer (Uniytinova-500, 500 and 125 MHz) using tetramethylsilane as the internal standard. The IR spectra of the cast films were obtained by a Perkin–Elmer 842 spectrometer. The T_g of PAGEC and PAGEC–silica were measured by a DSC (DuPont 2900) with a heating rate of 10 °C/min. The thermal degradation of PAGEC and PAGEC–silica and the silicon content of PAGEC–silica were measured by a TGA (DuPont 951). The scan rate was 20 °C/min from room temperature to 800 °C.

The molecular weight and its distribution were determined by a gel permeation chromatograph (Shimadzu LC-9A) using THF as the solvent and polystyrene as the standard. The element analyses (EA) were carried out in the Perkin–Elmer CHN 2400. The electron spectroscopy for chemical analysis system (ESCA) was carried out to analyze the silicon content of the PAGEC–$Si(OCH_3)_3$ precursor in the VG Scientific ESCALAB 250. The structure of PAGEC–silica was identified by a ^{29}Si-NMR (Bruker DSX-400WB). The elongation at break, tensile strength, and tensile modulus of the PAGEC and PAGEC–silica were measured in accordance with the ASTM test method D-638 (Instron Mini 44). The morphology of the fractured surface

Table 1
Copolymerization of AGE with CO_2 by various catalyst systems

Catalyst system I	 II	 III	Yield (g/(g of Zn))	$M_w \times 10^{-5}$	M_w/M_n
$Y(CF_3CO_2)_3$	$Zn(Et)_2$	Pyrogallol	25.2	4.90	3.70
–	$Zn(Et)_2$	Pyrogallol	23.6	4.43	4.44
$Y(CF_3CO_2)_3$	$Zn(Et)_2$	*m*-hydrobenzoic acid	–	–	–
$Y(CF_3CO_2)_3$	$Zn(Et)_2$	–	–	–	–
$Y(CF_3CO_2)_3$	–	Pyrogallol	–	–	–
$Y(CF_3CO_2)_3$	$Zn(Et)_2$	Glycerine	11.57	4.12	3.65

I = 0.0004 mol; II = 0.008 mol; III = 0.004 mol; solvent = 1,3-dioxolane of 30 ml; AGE = 30 ml; $T = 60$ °C; $P = 400$ psi; time = 12 h.

Table 2
Effect of the molar ratio of III to II on copolymerization of AGE with CO_2

Molar ratio III/II	Yield (g/(g of Zn))	$M_w \times 10^{-5}$	M_w/M_n
0.125	–	–	–
0.250	<0.5	–	–
0.500	25.2	4.90	3.70
0.750	20.4	4.56	4.35
1.000	15.5	4.02	4.56

I = 0.0004 mol; II = 0.008 mol; solvent = 1,3-dioxolane of 30 ml; AGE = 30 ml; $T = 60$ °C; $P = 400$ psi; time = 12 h.

Table 3
Effects of temperature and pressure on copolymerization of CO_2 and AGE

T (°C)	P (psi)	Yield, g of polymer/(g of Zn)	$M_w \times 10^{\times 5}$	M_w/M_n
50	400	14.8	4.17	4.99
60	400	25.2	4.90	3.70
70	400	22.0	2.91	3.77
80	400	1.9	2.56	4.13
60	100	13.9	3.36	5.96
60	300	18.7	4.23	4.25
60	500	22.9	3.92	4.78
60	600	20.1	3.02	5.85

I = 0.0004 mol; II = 0.008 mol; III = 0.004 mol; solvent = 1,3-dioxolane of 30 ml; AGE = 30 ml; time = 12 h.

of the PAGEC-silica was observed by the scanning electron microscope and Si-mapping photographs (Hitachi S-4700). The transparence was measured by the Hitachi U-3300. The wear loss and wear index were tested in accordance with the ASTM test method D4060-90 (PT3050 Taber).

3. Result and discussion

3.1. Synthesis and characterization of polyethercarbonate

Table 1 shows the experimental results for the copolymerization of CO_2 and AGE using different component III at 60 °C and 400 psi. It is seen that the catalyst system $Y(CF_3CO_2)_3$–$Zn(Et)_2$–pyrogallol offered the highest yield and molecular weight over the other systems. It is also seen that the copolymerization could proceed for the catalyst system $Zn(Et)_2$–pyrogallol and $Y(CF_3CO_2)_3$–$Zn(Et)_2$–glycerine, but not for the systems $Y(CF_3CO_2)_3$–$Zn(Et)_2$–*m*-hydrobenzoic acid, $Y(CF_3CO_2)_3$–$Zn(Et)_2$, and $Y(CF_3CO_2)_3$–pyrogallol, indicating that a proper choice of the catalyst component was essential and the active sites might be on zinc in the compound formed from the reaction between $Zn(Et)_2$ and pyrogallol or glycerine.

Table 2 shows the effect of the molar ratio of pyrogallol (III) to $Zn(Et)_2$ (II) on yield and the properties of the resultant copolymers when 0.0004 mol of the component $Y(CF_3CO_2)_3$ was used. The molar ratio of

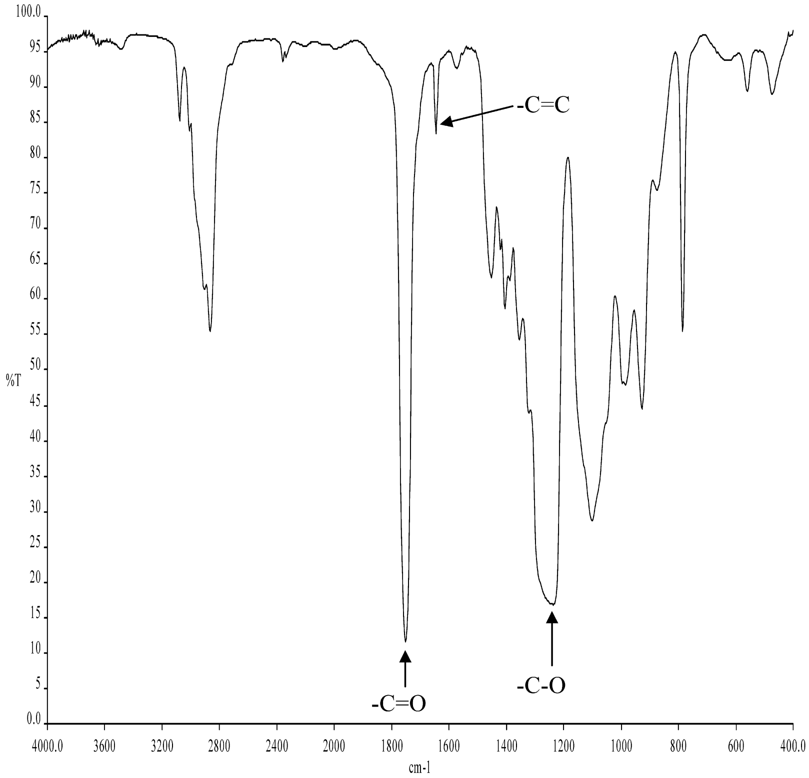

Fig. 1. The IR spectrum of the resulting copolymer synthesized from the copolymerization of AGE and CO_2. (Reaction conditions: I = 0.0004 mol; II = 0.008 mol; III = 0.004 mol; solvent = 1,3-dioxolane of 30 ml; AGE = 30 ml; $T = 60$ °C; $P = 400$ psi; time = 12 h).

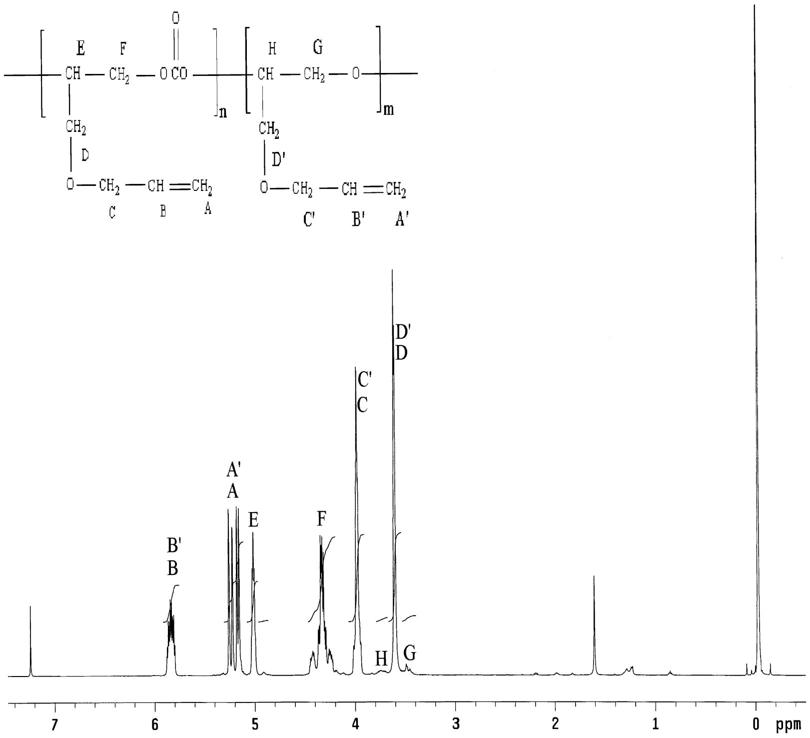

Fig. 2. The ^{1}H-NMR spectrum of the resulting copolymer synthesized from the copolymerization of AGE and CO_2. (Reaction conditions: I = 0.0004 mol; II = 0.008 mol; III = 0.004 mol; solvent = 1,3-dioxolane of 30 ml; AGE = 30 ml; T = 60 °C; P = 400 psi; time = 12 h).

pyrogallol to $Zn(Et)_2$ located at 0.5 was found to provide the highest yield and molecular weight as well as the narrowest molecular weight distribution. Table 3 shows that the most appropriate temperature and pressure regarding yield and molecular weight were located at about 60 °C and 400 psi, respectively. A decrease in yield with increasing temperature for the temperatures higher than 60 °C was probably due to the degradation of the resultant PAGEC. According to the transition state theory [16], reaction rate for a polymerization reaction is generally accelerated by pressure. For this copolymerization, the yield was increased with increasing pressure at

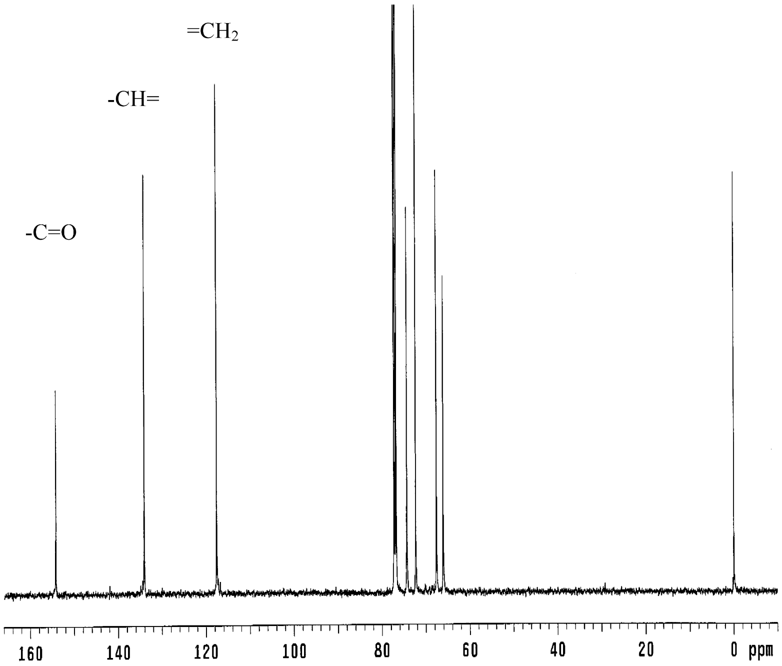

Fig. 3. The ^{13}C-NMR spectrum of the resulting copolymer synthesized from the copolymerization of AGE and CO_2. (Reaction conditions: I = 0.0004 mol; II = 0.008 mol; III = 0.004 mol; solvent = 1,3-dioxolane of 30 ml; AGE = 30 ml; T = 60 °C; P = 400 psi; time = 12 h).

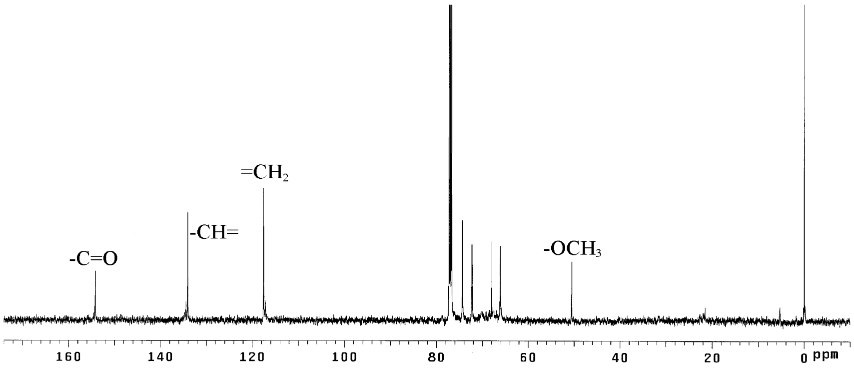

Fig. 4. The ^{13}C-NMR spectrum of the PAGEC–Si(OCH$_3$)$_3$ precursor.

pressures lower than 400 psi, but after that the yield was decreased with increasing pressure. A possible reason for a decrease in yield at higher pressures was due to a decrease in solubility of copolymer in the solvent resulting from the swelling of the solvent caused by the dissolution of CO_2. The existence of an optimum combination of temperature and pressure was also observed for the copolymerization of other epoxides with CO_2 [6,7].

The IR spectra of the resultant copolymer synthesized at the most appropriate operating conditions are shown in Fig. 1. The two absorption peaks at ca. 1250 and 1750 cm^{-1} provide an evidence for the presence of carbonate units in the resulting copolymer. The ^{1}H-NMR and ^{13}C-NMR spectra shown in Figs. 2 and 3 indicate that the copolymer was an alternating polyethercarbonate, just as for the synthesis of alternating polyethercarbonate from the copolymerization of CO_2 with propylene oxide and cyclohexene oxide [6,7]. From the element analysis, 53.7% of C and 6.63% of H were found in the generated PAGEC, equivalent to 97.7% of carbonate units present in the PAGEC. The calculated carbonate content was found to be close to that reported by Lukaszczyk et al. [15].

3.2. Identification of Si(OCH$_3$)$_3$-functionalized PAGEC precursor

The copolymer precursors were prepared by a free radical reaction of PAGEC with MSMA, VTES, or VTMS in the presence of the initiator BPO. From the ^{13}C-NMR shown in Fig. 4, it is observed that the functionalized group Si(OCH$_3$)$_3$ was grafted with PAGEC when MSMA was used. But it was not the case for VTES and VTMS using the initiators BPO and 2,2′-azobisisobutyronitrile (AIBN), indicating that only MSMA could react with PAGEC. The observed results verified the proposition that the reactivity of a silane monomer was small when the Si atom was sufficiently close to a vinyl group resulting from the presence of the dπ–pπ interactions between the Si atom and vinyl group [17]. It is also noted here that the generated

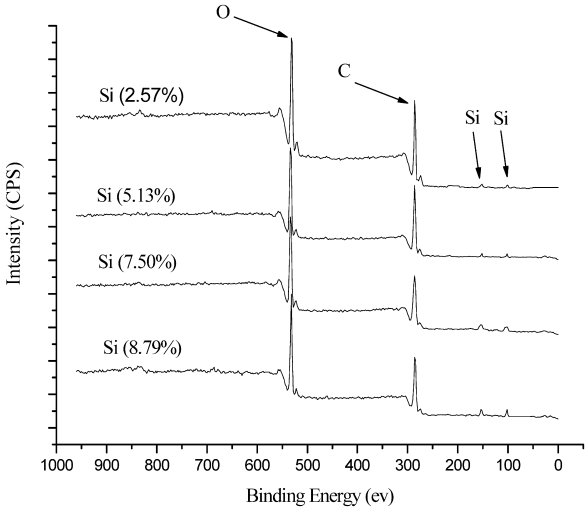

Fig. 5. The ESCA spectra of the PAGEC–Si(OCH$_3$)$_3$ precursors. (The Si contents at 2.57, 5.13, 7.50 and 8.79% were corresponding to the amounts of MSMA added in the preparation at 1.178, 2.358, 4.716 and 5.985 g, respectively).

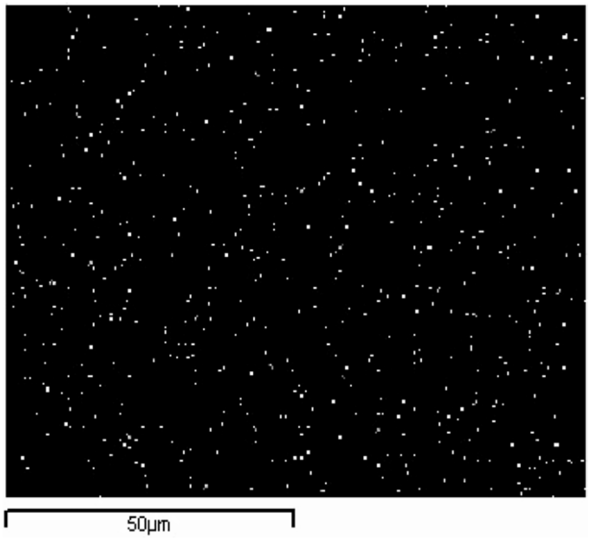

Fig. 6. The Si-mapping photograph of the copolymer precursor with the Si content of 5.13%.

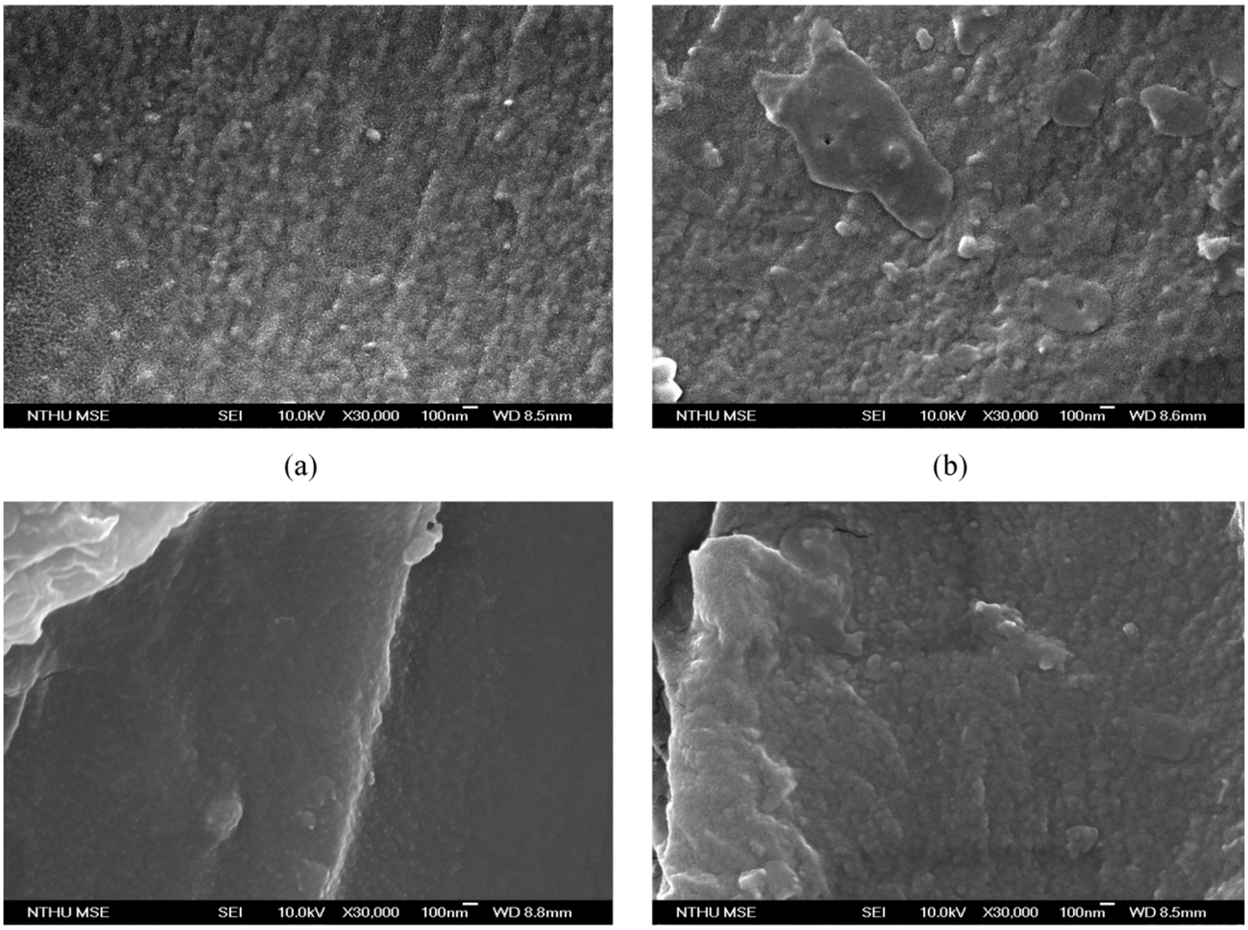

(a) (b)

(c) (d)

Fig. 7. The SEM photographs of the PAGEC–SiO_2 nanocomposites with different Si contents: (a) 2.6%, (b) 3.9%, (c) 6.6%, (d) 7.9%.

polymer from the reaction of PAGEC and MSMA was found not to be dissolved in hexane. It is known that MSMA monomer and $(MSMA)_n$ can be dissolved in hexane [17]. Under this situation, the different solubility in hexane provides another proof that the generated precursor after hexane purification was a copolymer rather than a mixture of two polymers. The ESCA plots shown in Fig. 5 indicate the presence of Si in the PAGEC precursor and an increased content of Si in the precursor with increasing the amount of MSMA in the preparation. Fig. 6 shows a uniform distribution of Si in the PAGEC precursor, providing an evidence other than the ^{1}H-NMR and ^{13}C-NMR spectra that the resultant PAGEC from the copolymerization of AGE with CO_2 was an alternating polyethercarbonate and the grafting of $Si(OCH_3)_3$ to PAGEC indeed occurred. The PAGEC precursor with the Si content of 5.13% determined by the ESCA was chosen in the preparation of the PAGEC–SiO_2 nanocomposites.

3.3. Characterization of PAGEC–SiO_2 nanocomposites

Figs. 7 and 8 are the SEM and Si-mapping photographs of the fractured surfaces of the PAGEC–SiO_2 nanocomposites generated by the addition of different amounts of TEOS in the sol–gel process. It can be seen that the SiO_2 particles were in a range of 50–100 nm and the size of SiO_2 was increased with increasing the added amount of TEOS. The uniform dispersion of Si in the PAGEC–SiO_2 nanocomposites indicates that silica networks were restrained under molecular level in the nanocomposites. Fig. 9 shows the ^{29}Si-NMR spectra of the PAGEC–$Si(OCH_3)_3$ precursors and PAGEC–SiO_2 nanocomposites. For the copolymer precursor PAGEC–$Si(OCH_3)_3$, there existed three types of silicon atom at about -48, -57 and

Table 4
The T_g and T_{10} of the synthesized nanocomposites with different Si contents

	TEOS (wt%)				
	0	9.1	16.7	23.1	28.6
Si (wt%)	0	2.6	3.9	6.6	7.9
T_g (°C)	-18	-8	-4	2	7
T_{10} (°C)	266	278	292	294	301

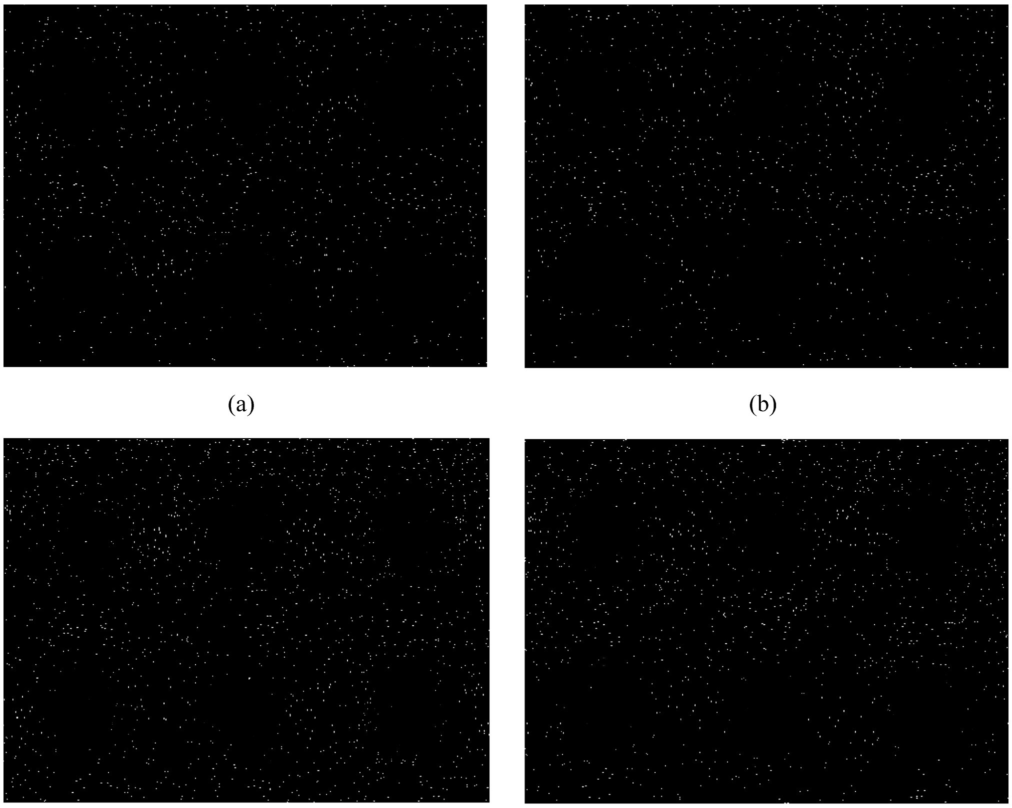

Fig. 8. The Si-mapping photographs of the PAGEC–SiO_2 nanocomposites with different Si contents: (a) 2.6%, (b) 3.9%, (c) 6.6%, (d) 7.9%.

− 65 ppm, designated as T^1, T^2, and T^3, respectively [18]. For the PAGEC–SiO_2 nanocomposites, there existed three types of silicon atom at about − 90, − 100 and − 110 ppm, designated Q^2, Q^3, and Q^4, respectively [18]. The obtained ^{29}Si-NMR spectra, therefore, verify the formation of silica network in the resultant nanocomposites.

Table 4 shows that the silicon content in the PAGEC–SiO_2 nanocomposite was increased with increasing the added amount of TEOS. As a result, the glass transition temperatures (T_g) of the PAGEC–SiO_2 nanocomposites was increased with increasing silicon content, indicating the hindrance to the motion of the large segments of PAGEC by a SiO_2 network. Table 4 also shows the T_{10} of the PAGEC-SiO_2 nanocomposites was varied significantly with the silicon content. It was increased from 266 to 301 °C for the silicon content was increased from 2.6 to 7.9%. The enhancement of the thermal stability might be attributed to the presence of an interaction force between PAGEC chains and silica network and a uniform distribution of silica in the PAGEC matrix.

Table 5 shows that both the tensile strength and tensile modulus of the PAGEC-SiO_2 nanocomposite were increased with increasing the content of TEOS and were higher than those of the PAGEC itself. Table 5 also shows that the elongation at break was decreased with increasing the content of TEOS, implying an improvement on mechanic strength after the incorporation of inorganic silica into the PAGEC matrix. Figs. 10 and 11 show that the wear loss and wear index of the PAGEC–SiO_2 were decreased with increasing the content of TEOS, indicating an improvement on the wear properties of the synthesized nanocomposites. The expected improvement was resulted

Table 5
The mechanical properties of the synthesized nanocomposites with different Si contents

Nanocomposite (Si content)	Tensile strength (MPa)	Tensile modulus (MPa)	Elongation at break (%)
PAGEC (0%)	1.9	93.2	15.9
PAGEC–SiO_2 (2.6%)	8.9	266.3	7.1
PAGEC–SiO_2 (3.9%)	11.1	310.7	6.2
PAGEC–SiO_2 (6.6%)	13.5	381.2	5.5
PAGEC–SiO_2 (7.9%)	16.3	439.3	5.0

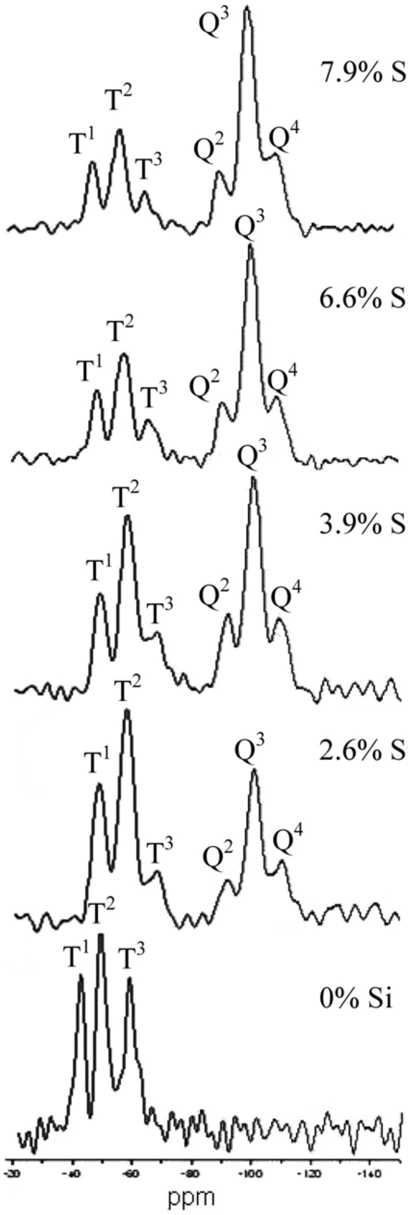

Fig. 9. The solid state ^{29}Si-NMR spectra of the PAGEC–SiO_2 nanocomposites with different Si contents.

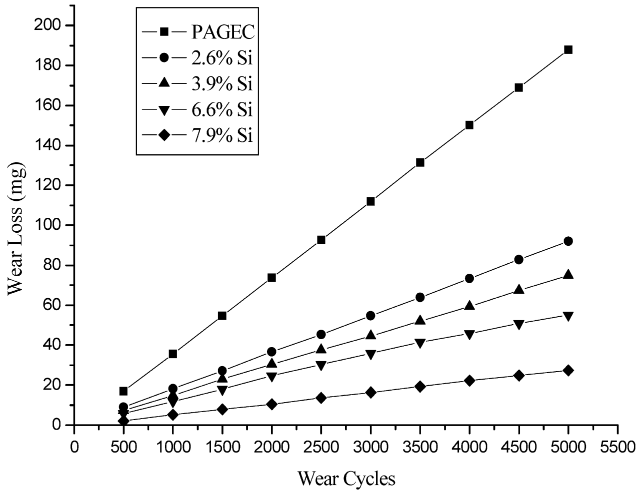

Fig. 10. The wear loss of the PAGEC–SiO_2 nanocomposites with different Si contents.

from the addition of inorganic SiO_2 into the PAGEC matrix. A constant wear index shown in Fig. 11 implies that the wear properties of the resultant nanocomposite were stable. Fig. 12 shows that the transparence of the resultant PAGEC–SiO_2 was slightly smaller than that of the PAGEC itself and could maintain a value higher than 85% at various contents of TEOS, providing the evidence that the silica particles were less than 100 nm and the distribution of Si atom was uniform in the PAGEC–SiO_2 nanocomposites.

4. Conclusions

An alternating polyethercarbonate could be effectively synthesized from the copolymerization of allyl glycidyl ether with CO_2 in the presence of the catalyst system $Y(CF_3CO_2)_3$–$Zn(Et)_2$–pyrogallol with the molar ratio of 1:20:10 in 1,3-dioloxane. The most appropriate operating conditions were found to be at 60 °C and 400 psi. The molecular weight of the resultant polyethercarbonate was as high as of 4.0×10^5 with a dispersity of 3.7 and the glass transition temperature was of -19 °C.

A PAGEC–SiO_2 nanocomposite in the based PAGEC was effectively synthesized via a sol–gel process. During the synthesis, only MSMA was found to react with PAGEC to result in a copolymer precursor for sol–gel process, but not for VTES and VTMS. The ESCA and Si-mapping show a uniform distribution of Si in the generated nanocomposite. Besides, a SiO_2 network structure with silica particles less than 100 nm in the nanocomposite was observed from the ^{29}Si-NMR, SEM, and Si-mapping. The thermal and mechanical properties of the PAGEC–SiO_2 nanocomposite,

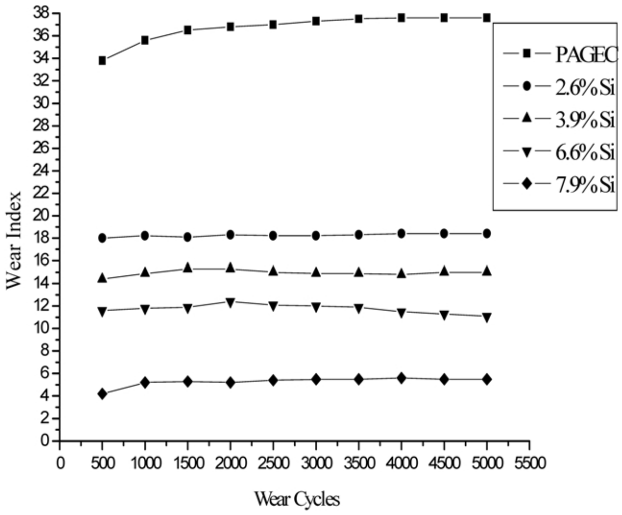

Fig. 11. The wear index of the PAGEC–SiO_2 nanocomposites with different Si contents.

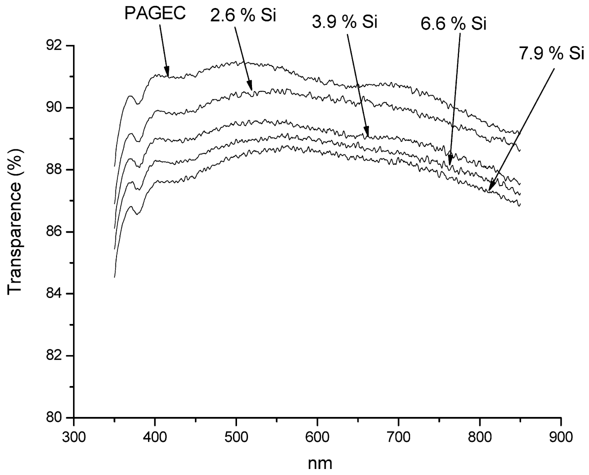

Fig. 12. The transparence of the PAGEC–SiO_2 nanocomposites with different Si contents.

including, T_g, T_{10}, tensile strength, tensile modulus, elongation at break, wear loss, and wear index, were found to be improved over the based PAGEC. Besides, the transparency of the resultant nanocomposite with different silica contents could be over 85%.

References

[1] Inoue S, Koinuma H, Tsuruta T. Makromol Chem 1969;130:210.
[2] Rokicki A, Kuran W. J Macromol Sci, Rev Macromol Chem 1981; C21:135.
[3] Scholsky KM. J Supercrit Fluids 1993;6:103.
[4] Wu J, Shen Z. J Polym Sci, Polym Chem 1990;28:1995.
[5] Chen X, Shen Z, Zhang Y. Macromolecules 1991;24:5305.
[6] Tan CS, Hsu TJ. Macromolecules 1997;30:3147.
[7] Hsu TJ, Tan CS. Polymer 2001;42:5143.
[8] Hsu TJ, Tan CS. Polymer 2002;43:4535.
[9] Morikawa A, Iyoku Y, Kakimoto M, Imai Y. J Mater Chem 1992;7: 679.
[10] Wei Y, Yang D, Tang L. J Mater Res 1993;8:1143.
[11] Landry CT, Coltrain BK, Brady BK. Polymer 1993;33:1486.
[12] Wen J, Wilkes GL. Chem Mater 1996;8:1667.
[13] McCarthy DW, Mark JE, Schaefer DW. J Polym Sci, Part B: Polym Phys 1998;36:1167.
[14] Schottner G. Chem Mater 2001;13:3422.
[15] Lukaszczyk J, Jaszcz K, Kuran W, Listos T. Macromol Rapid Commun 2000;21:754.
[16] Savage PE, Gopalan S, Mizan TI, Martino CJ, Brock EC. AIChE J 1995;41:1723.
[17] Rao VL, Babu GN. Eur Polym J 1989;25:605.
[18] Joseph R, Zhang S, Ford WT. Macromolecules 1996;29:1305.